Chemical Engineering Journal 214 (2013) 139–148

Contents lists available at SciVerse ScienceDirect

Chemical Engineering Journal

journal homepage: www.elsevier.com/locate/cej

Sequential precipitation of a new goethite–calcite nanocomposite and its possible application in the removal of toxic ions from polluted water

G. Montes-Hernandez [a,*], F. Renard [a,b], R. Chiriac [c], N. Findling [a], J. Ghanbaja [d], F. Toche [c]

[a] CNRS and University Grenoble 1, Institute of Earth Sciences (ISTerre), OSUG/INSU, BP 53, 38041 Grenoble Cedex 9, France
[b] Physics of Geological Processes, University of Oslo, Norway
[c] Université de Lyon, Université Lyon 1, Laboratoire des Multimatériaux et Interfaces, UMR CNRS 5615, 43 bd du 11 novembre 1918, 69622 Villeurbanne Cedex, France
[d] Université Henri Poincaré, Service Commun de Microscopies Electroniques et Microanalyses X, Bd. Des Aiguillettes, BP 239, 54506 Vandoeuvre-lès-Nancy, France

HIGHLIGHTS

- A simple and innovative synthesis route for goethite–calcite nanocomposite.
- Nanosized goethite particles adhered onto sub-micrometric calcite.
- Goethite–calcite composite has a well sequestration capacity for toxic ions.

ARTICLE INFO

Article history:
Received 13 July 2012
Received in revised form 26 October 2012
Accepted 27 October 2012
Available online 2 November 2012

Keywords:
Goethite
Calcite
Nanocomposite
Precipitation
Removal
Metalloids
Heavy metals

ABSTRACT

This study proposes a simple and innovative synthesis route for a goethite–calcite nanocomposite. This synthesis is summarised by three sequential precipitation reactions: (1) precipitation of nanosized acicular goethite (α-FeOOH) using a high OH/Fe molar ratio (=5); (2) instantaneous precipitation of portlandite ($Ca(OH)_2$) by adding $CaCl_2$ salt to a goethite alkaline suspension ($2NaOH + CaCl_2 \rightarrow Ca(OH)_2 + 2NaCl$) and; (3) sub-micrometric calcite precipitation by injection of CO_2 into a goethite–portlandite alkaline suspension ($Ca(OH)_2 + CO_2 \rightarrow CaCO_3 + H_2O$). The XRD patterns have confirmed the goethite and calcite mineral composition in the composite precipitated at 30 and 70 °C. FESEM and TEM observations have revealed the formation of nanosized goethite particles well dispersed with sub-micrometric calcite particles, leading to an orange–brown colour nanocomposite with high specific surface area of around 92 m^2/g for a composite synthesized at 30 °C and 45 m^2/g for a composite synthesized at 70 °C. Both values were determined using the conventional BET method on N_2 sorption isotherms. Finally, a goethite/calcite weight ratio equal to 0.8 in the composite was determined by Thermogravimetric Analysis (TGA). Additionally, some adsorption experiments carried out at two different pH values revealed that the goethite–calcite composite has a good sequestration capacity for Cu > Cd > As(III) > Se(IV) > As(V). Conversely, the Se(VI) did not show any chemical affinity with the goethite–calcite composite under the physico-chemical conditions studied. In practice, the goethite–calcite composite can neutralise acidic wastewater by slight calcite dissolution, enhancing the removal of heavy metals (e.g. Cu and Cd) at the calcite–solution interfaces.

1. Introduction

Goethite and calcite are two inorganic compounds that are widely studied due to their abundance in nature as minerals (abiotic origin) and biominerals (biotic origin). Both minerals can coexist in several terrestrial environments such as deep geological formations, water aquifers, soils and aerosols, and play a major role in the fate and transport of several metalloids and heavy metal trace elements and organic molecules at the mineral–fluid interfaces [1–5]. Goethite and calcite minerals have also been identified in several extraterrestrial environments. For example, calcite has recently been discovered in Martian soils by the Phoenix Mars exploration mission [6] and goethite has been suspected as a constituent of Martian dust and dark asteroids [7,8]. Moreover, goethite and calcite minerals are technologically important materials and widely applied as components in various industrial products, e.g., pigments in the building industry, inorganic dyes, pigments and adsorbents in the paper industry, lacquers or plastics, sorbents

* Corresponding author.
E-mail address: german.montes-hernandez@ujf-grenoble.fr (G. Montes-Hernandez).

1385-8947/$ - see front matter © 2012 Elsevier B.V. All rights reserved.
http://dx.doi.org/10.1016/j.cej.2012.10.050

in the removal of toxic ions and molecules from polluted water, active ingredient in antacid tablets [9–18]. In the last few decades, several synthesis routes have been proposed to produce goethite or calcite independently at laboratory or industrial scale, focusing on specific or multiple applications or simply to carry out basic research on the crystal growth processes [15,18–28]. Studies are continuing with a view to improving existing methods and/or developing innovative routes to obtain well-controlled shapes and sizes of nanometer-to-submicrometer goethite or calcite particles. Moreover, the nucleation and growth processes of goethite and calcite are still open subjects [24,25,29].

Several toxic ions, and particularly so-called oxyanions, are highly mobile in soils and groundwater since most natural minerals have net negative surface charges. Several inorganic oxyanions such as nitrates, chromates, arsenates, molybdates, selenites and selenates, can be toxic to humans or wildlife at μg/L–mg/L concentrations. Other oxyanions such as phosphates or nitrates can disturb the natural environment by amplifying eutrophication processes. Toxic ions can be removed from polluted water by coprecipitation [30,31], reverse osmosis [32], chemical reduction to less soluble species [33], and adsorbing colloid flotation (ACF) methods [34,35]. These methods generally need large facilities due to the various equipment and reagents used in the series of treatments involved. In addition, it is much more difficult to remove toxic oxyanions than cations because anions with a similar structure, such as nitrates, sulphates and phosphates often coexist at high concentrations in nature. Although processes of adsorptive removal of toxic oxyanions from solutions using conventional adsorbents, such as activated carbon [36,37], tanning gel [38], zeolites [39], iron oxides [40–43], and aluminium oxide [44], have been reported, they are not selective and sometimes have low effectiveness. Searching effective adsorbents, reagents and/or novel methods for the removal of the toxic ions still represents a major environmental remediation issue.

The present study proposes a simple and innovative synthesis route for a goethite–calcite nanocomposite. To the best of our knowledge, the synthesis of this composite has not been reported in the literature. This new nanocomposite could efficiently remove several metalloids and heavy metals (e.g. Cu(II), Cd(II), As(III), Se(IV), As(V), etc.) from synthetic polluted water and it offers a number of advantages as an adsorbent compared to pure goethite. For example, nanosized goethite particles generally form colloidal suspensions in mixed reactors and it becomes extremely difficult to separate the solid from the solution after water treatment by sorption. Conversely, in the goethite–calcite nanocomposite, the smaller goethite particles remain adhered to the calcite surfaces, thus providing a simpler and cheaper solid-solution separation process (e.g. by sedimentation and/or filtration). Another practical advantage is that the goethite–calcite composite can neutralise acidic wastewater by slight calcite dissolution during the sorption process, accentuating the removal of heavy metals (e.g. Cu and Cd) at the calcite–solution interfaces (this study).

This study has a twofold objective: firstly, propose a simple and innovative synthesis route for a goethite–calcite nanocomposite using a sequential reaction procedure, and secondly, provide some arbitrary adsorption experiments to evaluate its possible application in the removal of toxic ions from polluted water. The goethite–calcite composite was characterised by X-Ray Powder Diffraction (XRD), Field Emission Gun Scanning Electron Microscopy (FESEM), Transmission Electron Microscopy (TEM), N_2 adsorption isotherms and Thermogravimetric Analysis (TGA/SDTA). The concentrations the elements ([Ca], [Fe], [Na], [As], [Se], [Cd] and [Cu]) in filtered and acidified solutions from adsorption experiments were determined by inductively coupled plasma optical emission spectrometry (ICP-OES).

2. Materials and methods

2.1. Synthesis of goethite–calcite (stirred reactor)

One litre of high-purity water with electrical resistivity of 18.2 MΩ cm, 1 mol of NaOH and 0.2 mol of $FeCl_3.6H_2O$ were placed in a titanium reactor (autoclave with internal volume of 2 l). This aqueous reactive system was immediately stirred using constant mechanical agitation (400 rpm) during the reaction. The aqueous system was then heated at 30 °C or 70 °C for 24 h using a heating jacket adapted to the reactor. The autoclave was disassembled after 24 h and 30 g of $CaCl_2$ salt was added to the goethite alkaline suspension. The autoclave was rapidly assembled and the heating and agitation systems were re-started. For this case, the calcium chloride reacts instantaneously with the residual NaOH in the goethite suspension, leading to the formation of portlandite or calcium hydroxide particles ($2NaOH + CaCl_2 \rightarrow Ca(OH)_2 + 2NaCl$). When the reaction temperature was stabilised at 30 °C or 70 °C, CO_2 at 20 bar was injected into the goethite–portlandite suspension. A portlandite carbonation process immediately takes place ($Ca(OH)_2 + CO_2 \rightarrow CaCO_3 + H_2O$). Carbonation equilibrium (monitored by a drop in CO_2 pressure) was reached after about 8 h but the reaction was stopped after 24 h in both cases (i.e. at 30 °C and 70 °C).

At the end of the experiment, the autoclave was removed from the heating system and immersed in cold water when the experiment was carried out at 70 °C. After water cooling at 30 °C (about 10 min) the autoclave was disassembled, and the solid product was carefully recovered and separated by centrifugation (30 min at 12,000 rpm), decanting the supernatant solutions. The solid product from both syntheses (i.e. at 30 °C and 70 °C) was washed twice by re-dispersion/centrifugation processes in order to remove the halite (NaCl) co-precipitated during the synthesis. Finally, the solid product was dried directly in the centrifugation flasks at 60 °C for 48 h. The dry solid product was manually recovered, weighed and stored in plastic flasks for further characterisation (FESEM, TEM, XRD, TGA and N_2 sorption isotherms).

2.2. Characterisation of goethite–calcite composite

2.2.1. FESEM and TEM observations

Pure goethite and goethite–calcite composites were dispersed by ultrasonic treatment in absolute ethanol for 5–10 min. One or two droplets of the suspension were then deposited directly on an aluminium support for SEM observations, and coated with platinum. Morphological observations of various selected powders were performed using a Zeiss Ultra 55 field emission gun scanning electron microscope (FESEM) that has a maximum spatial resolution of approximately 1 nm at 15 kV. The composite dispersed by ultrasonic treatment in ethanol was also oriented on carbon Ni grids and then imaged using a JEOL 3010 Transmission Electron Microscope (TEM) equipped with an energy dispersive X-ray analyzer (EDS).

2.2.2. XRD measurements

X-ray Powder Diffraction (XRD) analyses were performed using a D5000, SIEMENS diffractometer in Bragg–Brentano geometry, equipped with a theta–theta goniometer with a rotating sample holder. The XRD patterns were collected using Cu $K\alpha_1$ ($\lambda_{k\alpha1}$ = 1.5406 Å) and $K\alpha_2$ ($\lambda_{k\alpha2}$ = 1.5444 Å) radiation in the range 2θ = 10–70° with a step size of 0.04° and a counting time of 6 s per step.

2.2.3. Thermogravimetric analyses

TGA for goethite–calcite composites were performed with a TGA/SDTA 851^e Mettler Toledo instrument under the following

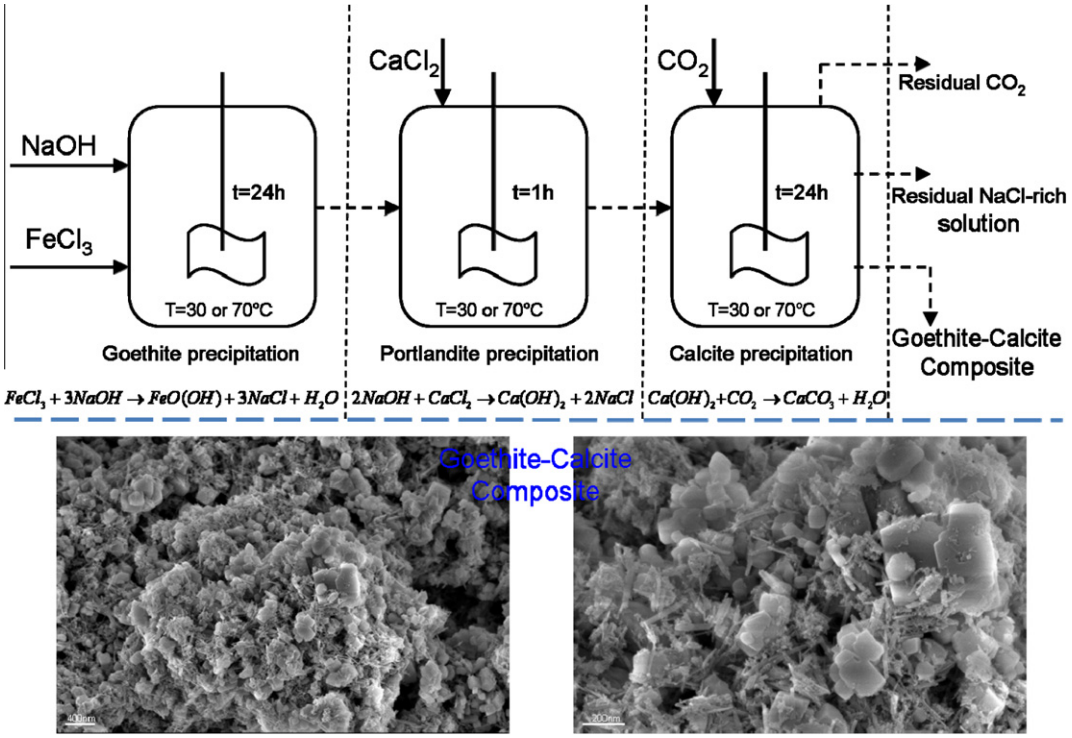

Fig. 1. Schematic diagram of sequential precipitation reactions for the synthesis of a goethite–calcite composite, including two FESEM images of the composite synthesised at 30 °C (two different magnifications).

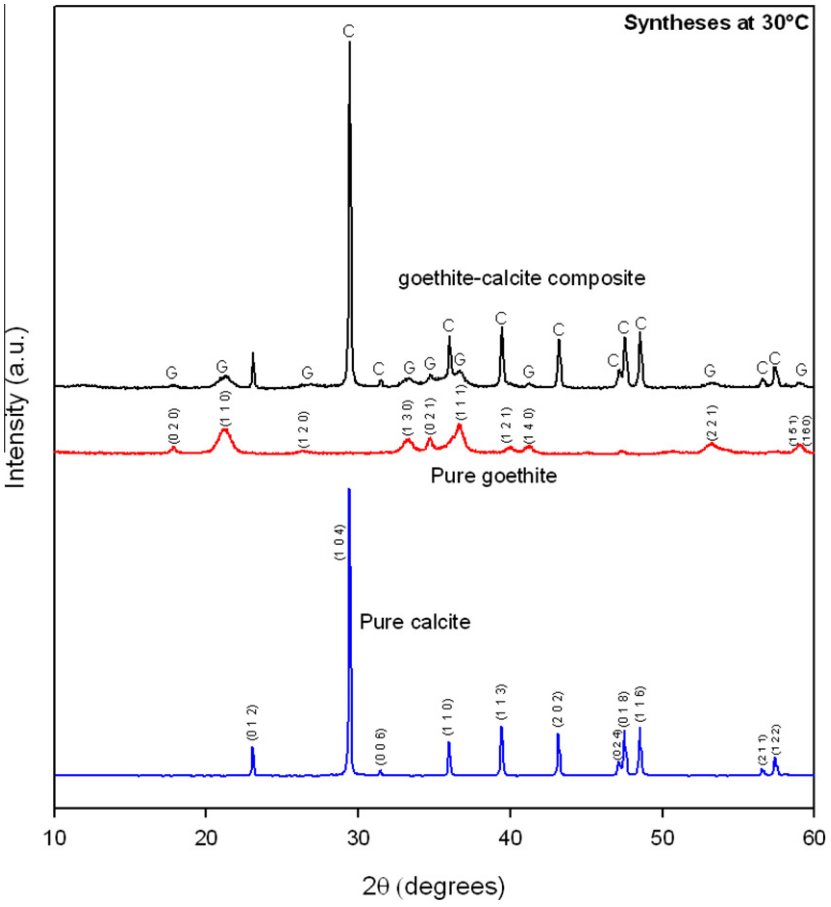

Fig. 2. X-ray diffraction (XRD) patterns of pure goethite, pure calcite and a goethite–calcite composite synthesised at 30 °C. Pure calcite and goethite were indexed from XRD patterns 005-0586 and 081-0464, respectively. G: goethite and C: calcite.

conditions: sample mass of about 10 mg, alumina crucible of 150 μl with a pinhole, heating rate of 10 °C min^{-1}, and inert N_2 atmosphere of 50 ml min^{-1}. Sample mass loss and associated thermal effects were obtained by TGA/SDTA. In order to identify the different mass loss steps, the TGA first derivative (rate of mass loss) was used. TGA apparatus was calibrated in terms of mass and temperature. Calcium oxalate was used for the sample mass calibration. The melting points of three compounds (indium, aluminium and copper) obtained from the DTA signals were used for sample temperature calibration.

2.2.4. N_2 sorption isotherms

N_2 sorption isotherms for goethite–calcite composites were determined using a sorptomatic system (Thermo Electron Corporation). The specific surface area of powdered samples was estimated by applying the Brunauer–Emmet–Teller (BET) equation in the $0.05 \leqslant P/P_0 \leqslant 0.35$ interval of relative pressure and using a value of 16.2 $Å^2$ for the cross-sectional area of molecular N_2. A non-linear regression by the least-squares method was performed to fit the interval data (n_{ads} vs. P/P_0) in the experimental isotherms. Additionally, the Barrett–Joyner–Halenda (BJH) method that takes into account the capillary condensation via the Kelvin equation, was used to determine pore size distribution.

2.3. Adsorption experiments in a semi-continuous mixed reactor

One litre of solution containing simultaneously two ions (As(III)-Se(IV), As(V)-Se(VI) or Cd(II)-Cu(II): about 50 mg/L for each ion) and 3 g of goethite–calcite composite was placed in a titanium reactor (autoclave with internal volume of 2 l). This suspension was immediately stirred using constant mechanical agitation (400 rpm) during the adsorption process at room temperature (≈20 °C). Subsequently, 15 ml of reacting suspension was withdrawn from the reactor as a function of time (0.16, 0.5, 1, 2, 3 and 24 h). For this case, the pH was measured in the suspensions at room temperature. The suspensions were then filtered through

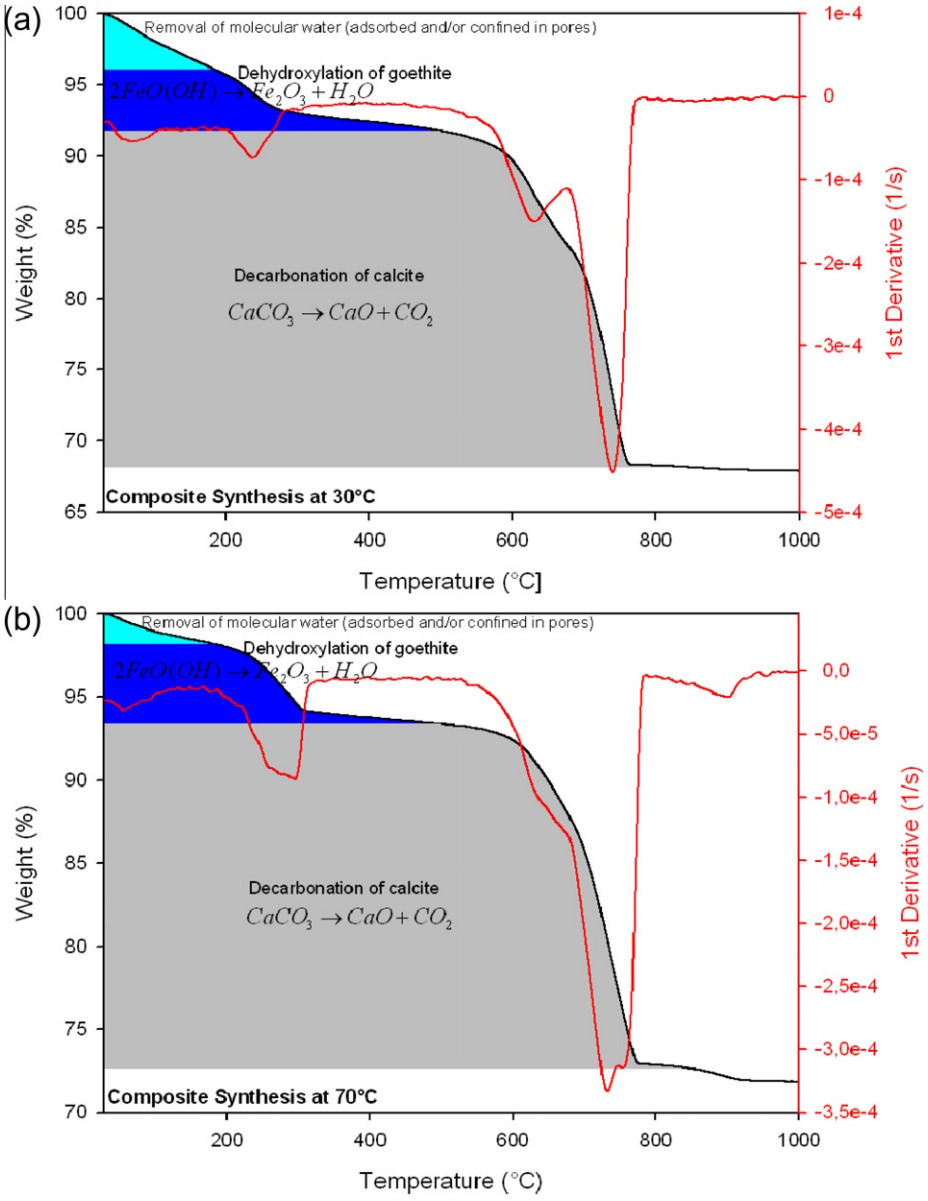

Fig. 3. Thermogravimetric analyses for goethite–calcite composites synthesised at 30 °C (a) and at 70 °C (b), including in both cases the first derivative curve (or differential themogravimetric analysis).

a 0.2 μm Teflon filter. 10 ml of the resulting filtered solutions was acidified for measurement of [Ca], [Fe], [Na], [As], [Se], [Cd] and [Cu] by inductively coupled plasma optical emission spectrometry (ICP-OES). In these adsorption experiments only the goethite–calcite composite synthesized at 30 °C was used because it has a higher specific surface area (92 m^2/g).

3. Results and discussion

3.1. Precipitation reactions

The goethite–calcite nanocomposite synthesis is summarised by three sequential precipitation reactions:

(1) Fast precipitation of nanosized acicular goethite (α-FeOOH) using a high OH/Fe molar ratio (=5).
(2) Instantaneous precipitation of portlandite ($Ca(OH)_2$) by adding $CaCl_2$ salt to the goethite alkaline suspension.
(3) Sub-micrometric calcite precipitation by injection of CO_2 into goethite–portlandite alkaline suspension.

Fig. 1 shows a schematic representation of goethite–calcite synthesis, summarising the three sequential precipitation reactions. These three steps are detailed below.

In a previous study [29], it was demonstrated that acicular goethite (α-FeOOH) can be precipitated when a high initial OH/Fe molar ratio (=5) and moderate temperature (30 °C and 70 °C) are used, without the need to synthesise ferrihydrite and/or amorphous iron hydroxide precursors. The goethite formation described here is characterised by the presence of three successive pH domains, that are specifically associated with (I) the formation of ferric hydroxide gel (FeH gel), leading to acid conditions (pH < 2.5); (II) the spontaneous nucleation of goethite from FeHgel, leading to alkaline conditions (pH > 11), and (III) the growth of goethite in alkaline conditions (11 < pH < 13.5). These three steps or pH domains during goethite formation are well correlated with changes in colour [29] and the overall reaction implying the three above steps can be written as:

$$FeCl_3 + 3NaOH \rightarrow FeO(OH) + 3NaCl + H_2O \quad (1)$$

Table 1
Average size of single goethite and calcite crystals measured on 50 isolated particles from FESEM images and specific surface area of goethite–calcite composites determined from N_2 adsorption isotherms.

Synthesis	Temperature (°C)	FESEM			S_{BET}
		Goethite		Calcite	
		Length (nm)	Width (nm)	Diagonal (nm)	
G-C30C	30	240 ± 40	40 ± 8	190 ± 30	92 m^2/g
G-C70C	70	700 ± 90	75 ± 20	500 ± 40	45 m^2/g

In our system, the goethite grows in alkaline conditions after spontaneous nucleation from ferric hydroxide gel because an excess of sodium hydroxide (NaOH) was initially imposed in the system. The residual NaOH after goethite formation was used to produce portlandite instantaneously by adding the calcium chloride ($CaCl_2$) to the goethite alkaline suspension. The overall reaction of portlandite precipitation ($Ca(OH)_2$), well known in the laboratory and at industrial scales [15,45], can be expressed as:

$$2NaOH + CaCl_2 \rightarrow Ca(OH)_2 + 2NaCl \quad (2)$$

Calcite precipitation or portlandite carbonation is the final step in the synthesis of goethite–calcite nanocomposites. For this case, CO_2 gas was directly injected into the portlandite–goethite alkaline suspension. CO_2 dissolution in alkaline conditions ($CO_2 + H_2O \rightarrow CO_3^{2-} + 2H^+$) produces a simultaneous consumption/dissolution of calcium hydroxide ($Ca(OH)_2 \rightarrow Ca^{2+} + 2OH^-$), leading to the precipitation of sub-micrometric calcite until a thermodynamic equilibrium between calcite–solution–CO_2 is obtained [24,46]. The overall aqueous carbonation reaction of calcium hydroxide or calcite precipitation can be expressed as:

$$Ca(OH)_2 + CO_2 \rightarrow CaCO_3 + H_2O \quad (3)$$

This neutralisation reaction implies a decrease in pH from 12.2 to 6.5 in the solution which did not promote the dissolution of pre-existing goethite because this mineral is stable in a broad range of pH values (3–13.5) [9,10,12].

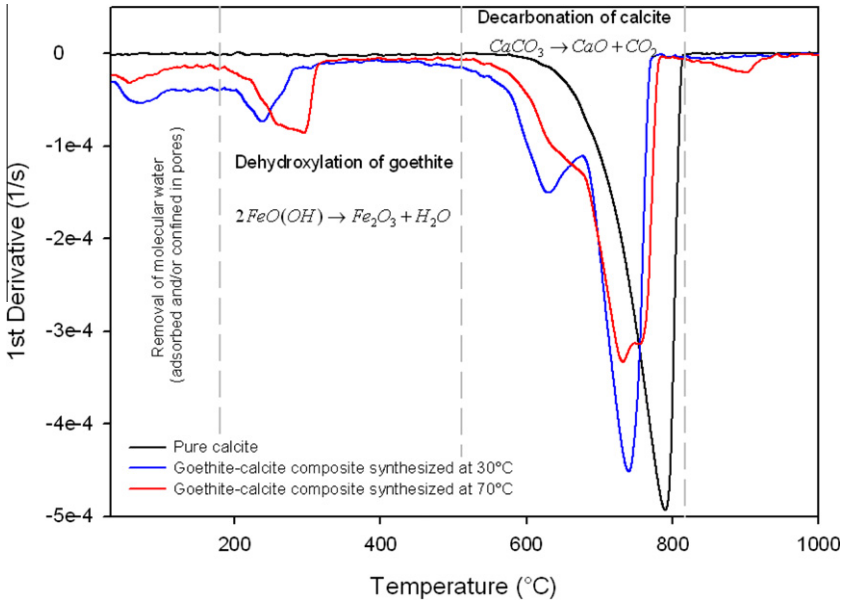

Fig. 4. First derivative TG curves (DTG) for pure calcite and goethite–calcite composites showing complex decarbonation of the calcite contained in the composites.

3.2. Characterisation of composite

The XRD measurements confirmed the goethite and calcite mineral composition in the composite precipitated at 30 °C and 70 °C. For example, the experimental XRD patterns obtained successfully matched with the ICDD cards #005-0586 for calcite and #081-0464 for goethite as shown in Fig. 2. These results were also evidenced by TGA. For this case, the 1st derivative curve, which corresponds to the rate of weight loss, clearly shows two major dehydration episodes, with the desorption of molecular water and the goethite dehydroxylation processes peaking between 55 and 70 °C and between 225 and 280 °C, respectively. The calcination or de-carbonation of calcite ($CaCO_3 \rightarrow CaO + CO_2$) takes place at higher temperature and two or three decarbonation episodes were identified between 570 and 770 °C (Fig. 3). Conversely, the pure calcite that was synthesised via reactions (2) and (3) was characterised by a single decarbonation episode peaking at a temperature close to 800 °C (see Fig. 4). This disagreement can be explained by the different size populations of calcite particles in the composite and possibly also by the presence of a small amount of amorphous calcium carbonate with lower thermal stability. Finally, based on TGA, a goethite/calcite weight ratio equal to 0.8 was determined in the composite. Complementary FESEM and TEM observations/measurements revealed nanosized goethite particles well dispersed and/or aggregated with sub-micrometric calcite particles. A small proportion of poorly-crystallized particles (possibly amorphous calcium carbonate) were also observed by TEM. However, no clear evidence of the presence of amorphous calcium carbonate was found. The average particle sizes (length and width for goethite and diagonal dimension for calcite) measured on 50 isolated particles are summarised in Table 1. This mineral mixture forms a homogeneous orange–brown nanocomposite with high

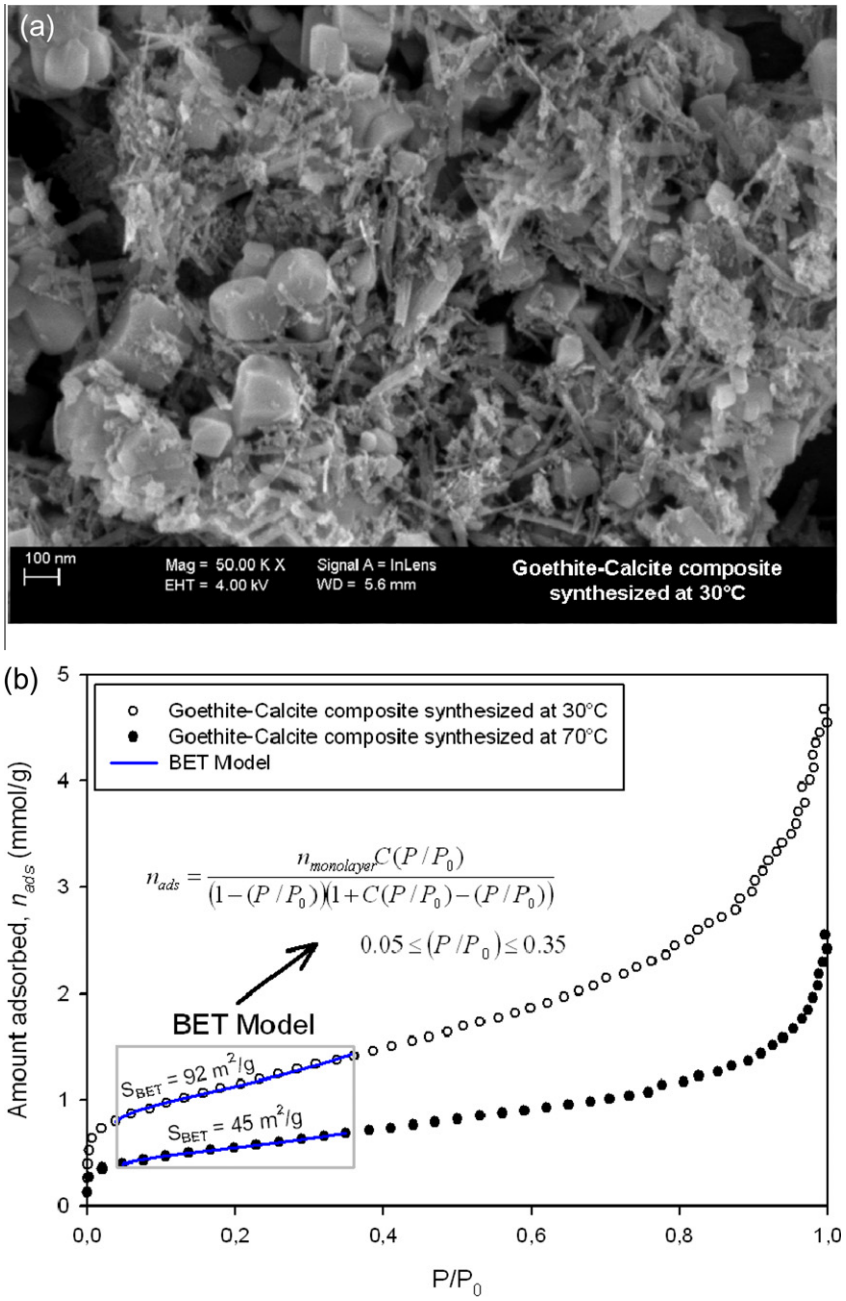

Fig. 5. (a) FESEM image showing nanosized and sub-micrometric particles of goethite and calcite. (b) N_2 experimental sorption isotherms for goethite–calcite composites synthesised at 30 °C and 70 °C and BET model fitting the experimental data between 0.05 and 0.35 of relative pressure.

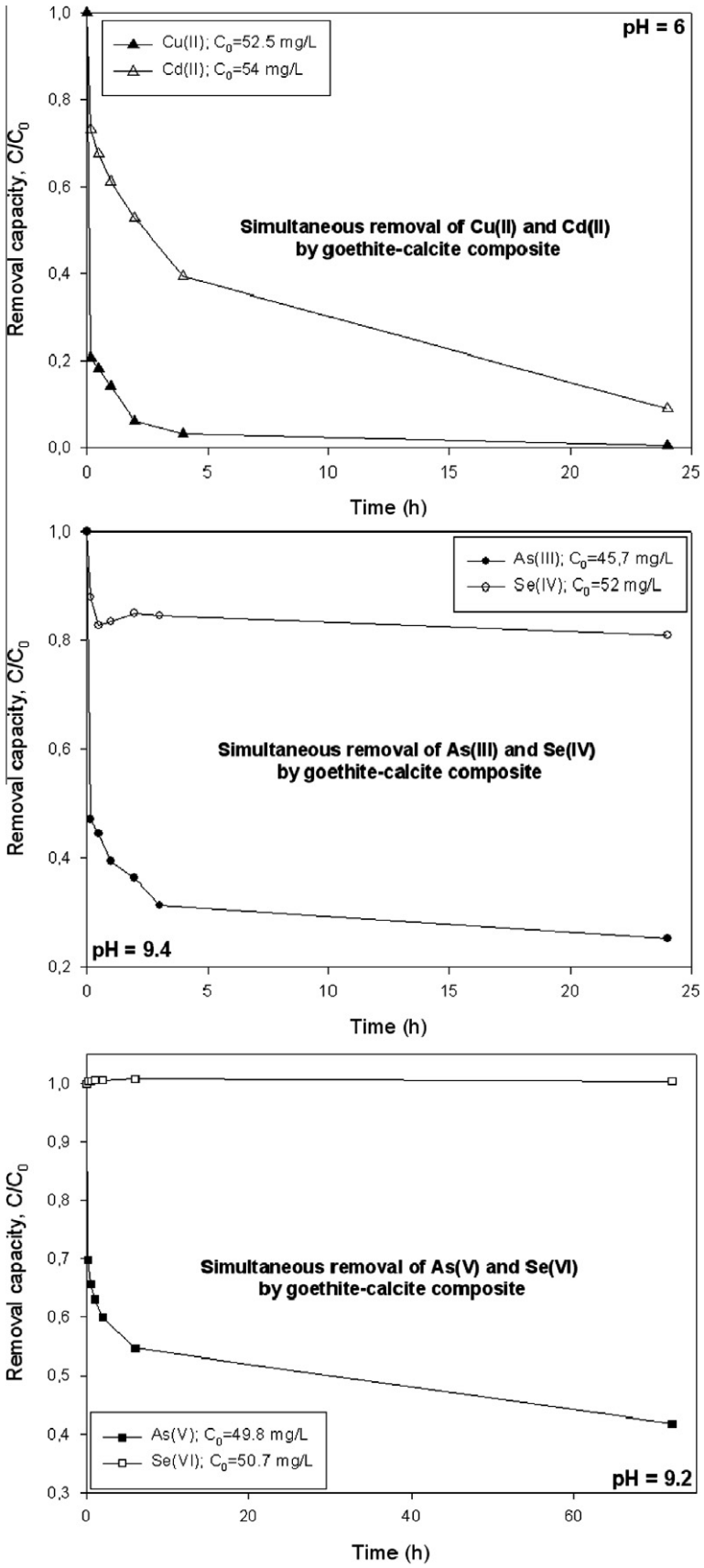

Fig. 6. Simultaneous removal of two toxic ions (i.e. binary-element systems) from synthetic wastewater via a sorption process on a goethite–calcite composite. Three different binary-ions systems are reported (top panel: Cu^{2+}–Cd^{2+}, middle panel: arsenite–selenite and bottom panel: arsenate–selenate).

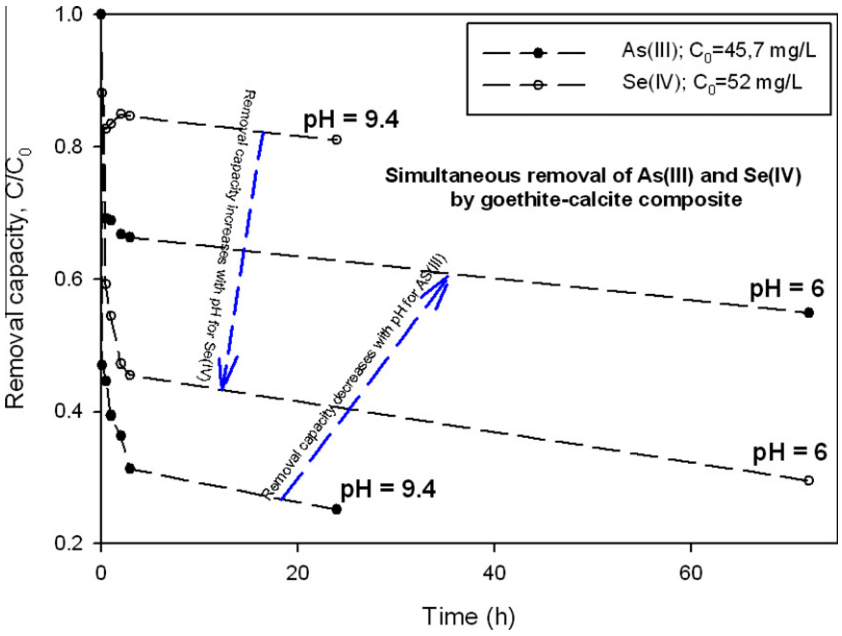

Fig. 7. pH effect on the simultaneous removal of arsenite (As(III) and selenite (Se(IV) from water using the goethite–calcite composite as sorbent.

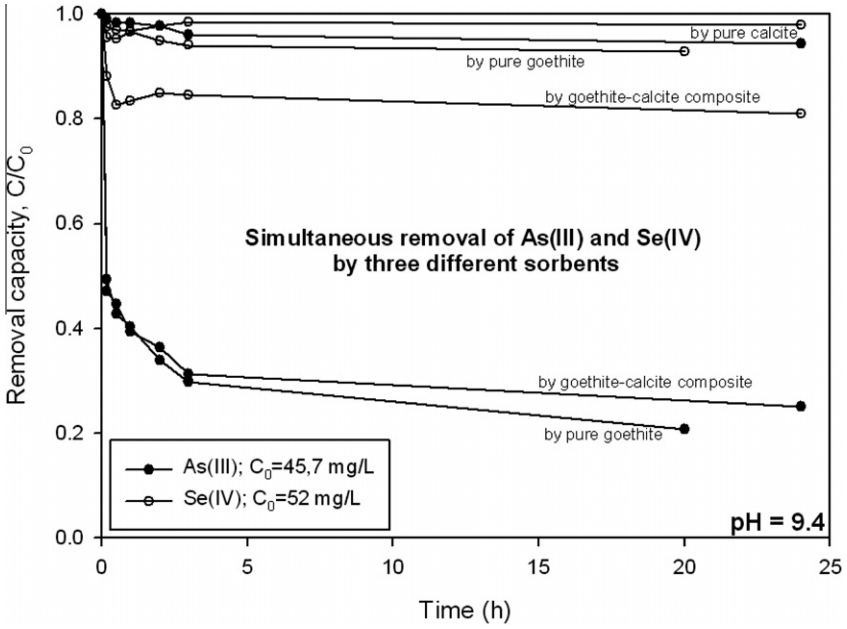

Fig. 8. Simultaneous removal of arsenite (As(III)) and selenite (Se(IV)) from water using the goethite–calcite composite, pure goethite and pure calcite.

specific surface area equal to 92 and 45 m^2/g for composites synthesized at 30 °C and 70 °C, respectively (Fig. 5). Moreover, both composites synthesised at different temperatures are mesoporous materials as determined from the BJH method. Pore size distribution here was in a short range of pore sizes from 2 to 20 nm (median pore radius = 6 nm) for the composite synthesised at 30 °C and from 2 to 30 nm (median pore radius = 9 nm) for the composite synthesised at 70 °C.

3.3. Toxic ion removal capacity

Additional adsorption experiments in a semi-continuous reactor and ICP-OES measurements revealed that the goethite–calcite composite has a good capacity for removing Cu > Cd > As(III) > Se(IV) > As(V) in the pH range from 6 to 10. Note that only two different pH values were investigated. Conversely, Se(VI) did not present any chemical affinity with the goethite–calcite composite under the physicochemical conditions studied. Pure goethite and calcite were also inefficient adsorbents for removing the Se(VI) from water under the same physico-chemical conditions. Fig. 6 summarises the simultaneous removal of three different binary-element systems using the goethite–calcite composite as adsorbent. An adsorption competition and a different chemical affinity for the six toxic ions (selenite, selenate, arsenite, arsenate, cadmium and copper) were clearly observed under the physico-chemical conditions investigated. Several studies demonstrated that pH plays a major role in the ion and molecule sorption process because the surface of the adsorbents (e.g. minerals) can be charged positively

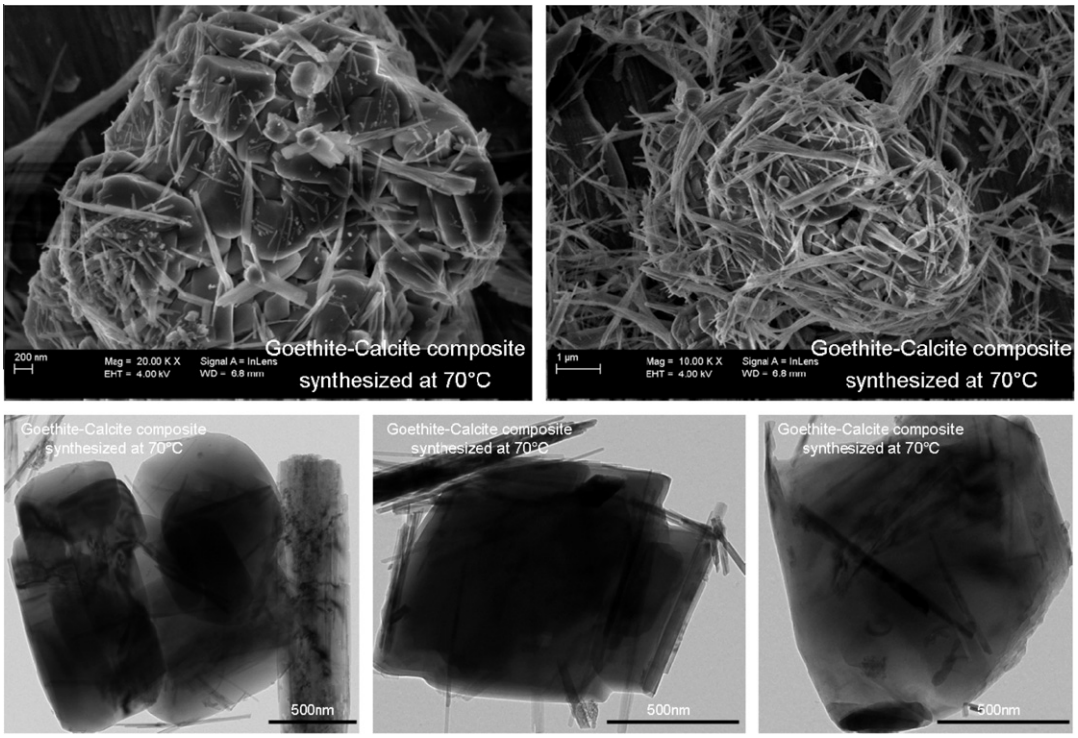

Fig. 9. FESEM and TEM images showing intimate cohesion/aggregation between goethite and calcite particles in the composite synthesised at 70 °C.

or negatively as a function of the pH and ionic strength of a given solution [1,47]. In our study, the removal of As(III) was promoted with respect to Se(IV) at alkaline pH (pH = 9.4). Conversely, the removal of Se(IV) was promoted with respect to As(III) at slight acidic pH (pH = 6) (Fig. 7). Finally, it was demonstrated that the ion removal capacity of the goethite–calcite composite was better or equivalent compared to pure goethite (Fig. 8), with the main improvement being that the nanocomposite is easier to separate from the fluid because of the aggregation of goethite with calcite particles. This aggregation process is determined by the balance of electrostatic forces, van der Waals forces and steric interactions at the nanoparticle–fluid interfaces. It may be speculated that the aggregation is controlled mainly by electrostatic forces because the surface charges of goethite and calcite change significantly during the three steps of our synthesis route [1,47], allowing goethite particle aggregation/cohesion on the calcite surfaces (Fig. 9). Another major advantage is that the goethite–calcite composite can neutralise acidic wastewater by slight calcite dissolution, thus improving the removal of heavy metals (e.g. Cu and Cd) at the solid-solution interfaces, with a preferential chemical affinity on calcite surfaces, as clearly observed in Fig. 10 for cadmium and copper.

4. Conclusion

In summary, a simple and novel synthesis route for goethite–calcite nanocomposite is proposed. Remarkably, this nanocomposite offers various advantages as an adsorbent for toxic elements (metalloids and heavy metals) compared to pure goethite. For example, the nanosized goethite particles generally form colloidal suspensions in mixed reactors, and in such case it becomes extremely difficulty to separate the solid from the solution after water treatment by sorption. In our case, the smaller goethite particles adhere to the calcite surfaces, thus allowing a simpler solid-solution separation process (e.g. sedimentation and/or filtration). Moreover, the goethite–calcite composite can neutralise acidic wastewater by slight calcite dissolution, thereby improving the re-

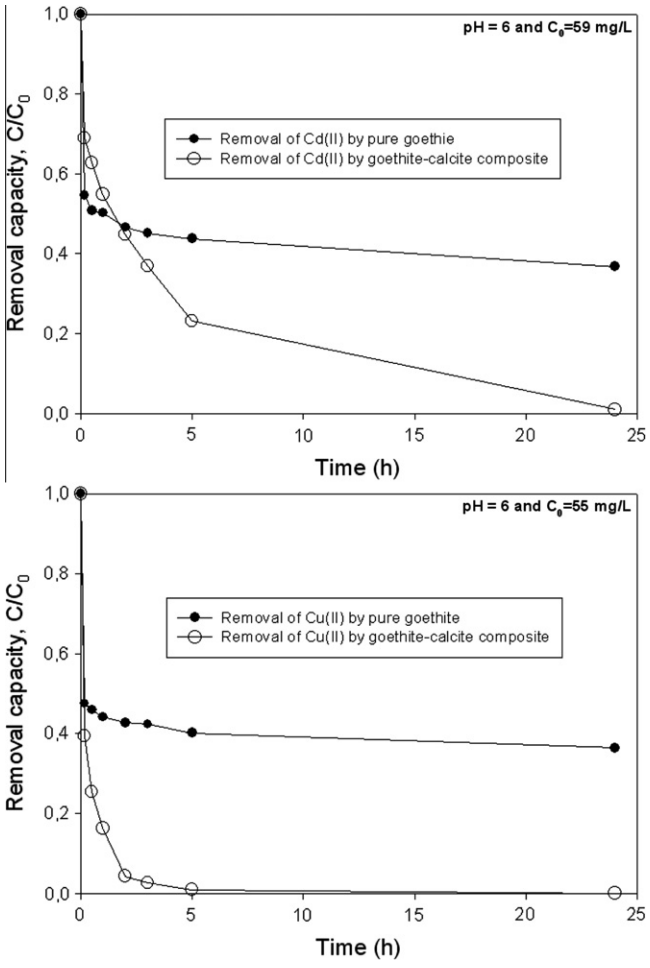

Fig. 10. Removal of Cd(II) and Cu(II) from solutions by pure goethite and goethite–calcite composite. Note that Cd and Cu are almost completely removed from solutions when the goethite–calcite composite was used.

moval of heavy metals (e.g. Cu and Cd) at the solid-solution interfaces, with a preferential chemical affinity on calcite surfaces. In general, the goethite–calcite nanocomposite was found to have a greater or equivalent capacity for the removal of metalloids and heavy metals compared to the pure goethite.

Acknowledgement

The authors are grateful to the National Research Council (CNRS), France, for providing a financial support for this work.

References

[1] M. Wolthers, L. Charlet, P. Van Cappellen, The surface chemistry of divalent metal carbonate minerals, Am. J. Sci. 308 (2008) 905–941.
[2] J. Paquette, R.J. Reeder, Relationship between surface structure, growth mechanism, and trace element incorporation in calcite, Geochem. Cosmochem. Acta 59 (1995) 735–749.
[3] A.J.A. Aquino, D. Tunega, G. Haberhauer, M.H. Gerzabek, H. Lischka, Acid-base properties of a goethite surface model. A theoretical view, Geochem. Cosmochem. Acta 72 (2008) 3587–3602.
[4] R.M. Cornell, U. Schwertmann, The Iron Oxides, VCH, Weinheim Germany, 1996.
[5] O. Ozdemir, D.J. Dunlop, Intermediate formation of magnetite during dehydration of goethite, Earth Planet Sci. Lett. 177 (2000) 59–67.
[6] W.V. Boynton, D.W. Ming, S.P. Kounaves, S.M.M. Young, R.E. Arvidson, M.H. Hecht, J. Hoffman, P.B. Niles, D.K. Hamara, R.C. Quinn, P.H. Smith, B. Sutter, D.C. Catling, R.V. Morris, Evidences for calcium carbonate at the Mars Phoenix landing site, Science 325 (2009) 61–64.
[7] R.V. Morris, G. Klingelhofer, C. Schroder, D.S. Radianor, A. Yen, D.W. Ming, P.A. De Souza, I. Fleischer, T. Wdowiak, R. Gellert, B. Bernhardt, E.N. Evlanov, B. Zubkov, J. Foh, U. Bonnes, E. Kankeleit, P. Gutlich, F. Renz, S.W. Squyres, R.E. Arvidson, Mösbauer mineralogy of rock soil dust at Gusev Crater Mars, J. Geophys. Res. 111 (2006) E02S13.
[8] P. Beck, E. Quirico, D. Sevestre, G. Montes-Hernandez, A. Pommerol, B. Schmitt, Goethite as an alternative origin for the 3.1 micro-m band on dark asteroids, Astron. Astrophys. (2010), http://dx.doi.org/10.1051/0004-6361/201015851.
[9] N.O. Núñez, P. Tartaj, M. Puerto Morales, R. Pozas, M. Ocaña, C.J. Serna, Preparation of high acicular and uniform goethite particles by modified-carbonate route, Chem. Mater. 15 (2003) 3558–3563.
[10] U. Schwertmann, R.M. Cornell, Iron Oxides in the Laboratory: Preparation and Characterization, VCH, Weinheim, Germany, 1991.
[11] M. Kosmulski, S. Durand-Vidal, E. Maczka, J.B. Rosenholm, Morphology of synthetic goethite particles, J. Colloid Interface Sci. 271 (2004) 261–269.
[12] D.M.E. Thies-Weesie, J.P. Hoog, M.H. Hernandez Mendiola, A.V. Petukhov, G.J. Vroege, Synthesis of goethite as a model colloid for mineral liquid crystals, Chem. Mater. 19 (2007) 5538–5546.
[13] M. Kosmulski, E. Maczka, E. Jartych, J.B. Rosenholm, Synthesis and characterization of goethite and goethite–hematite composite, Adv. Colloid Interface Sci. 103 (2003) 57–76.
[14] Garcia-Carmona, J. Gomez-Morales, J. Fraile-Sainz, R. Rodriguez-Clemente, Morphological characteristics and aggregation of calcite crystals obtained by bubbling CO_2 through a $Ca(OH)_2$ suspension in the presence of additives, Powder Technol. 130 (2003) 307–315.
[15] C. Domingo, E. Loste, J. Gomez-Morales, J. Garcia-Carmona, J. Fraile, Calcite precipitation by a high-pressure CO_2 carbonation route, J. Supercrit. Fluids 36 (2006) 202–215.
[16] C. Domingo, J. Garcia-Carmona, E. Loste, A. Fanovich, J. Fraile, J. Gomez-Morales, Control of calcium carbonate morphology by precipitation in compressed and supercritical carbon dioxide media, J. Crystal Growth 271 (2004) 268–273.
[17] G. Montes-Hernandez, A. Fernandez-Martinez, L. Charlet, D. Tisserand, F. Renard, Textural properties of synthetic calcite produced by hydrothermal carbonation of calcium hydroxide, J. Crystal Growth 310 (2008) 2946–2953.
[18] H.S. Lee, T.H. Ha, K. Kim, Fabrication of unusually stable amorphous calcium carbonate in an ethanol medium, Mater. Chem. Phys. 93 (2005) 376–382.
[19] A. Abou-Hassan, O. Sandre, S. Neveu, V. Cabuil, Synthesis of goethite by separation of the nucleation and growth process of ferrihydrite nanoparticles using microfluidics, Angew. Chem. 121 (2009) 2378–2381.
[20] T. Yu, J. Park, J. Moon, K. An, Y. Piao, T. Hyeon, Synthesis of uniform goethite nanotubes with parallelogram cross section, J. Am. Chem. Soc. 129 (2007) 14558–14559.
[21] Schwertmann, P. Cambier, E. Murad, Properties of goethite of varying crystallinity, Clays Clay Miner. 33 (1985) 369–378.
[22] M. Mohapatra, S.K. Gupta, B. Satpati, S. Anand, B.K. Mishra, pH and temperature dependent facile precipitation of nano-goethite particles in $Fe(NO_3)_3$–NaOH–$NH_3NH_2HSO_4$–H_2O medium, Colloids Surf. A: Physicochem. Eng. Asp. 355 (2010) 53–60.
[23] K.F. Hayes, A.L. Roe, G.E. Brown Jr., K.O. Hodgson, J.O. Leckie, G.A. Parks, In situ X-ray absorption study of surface complexes: selenium oxyanions on α-FeOOH, Science 238 (1987) 783–786.
[24] G. Montes-Hernandez, F. Renard, N. Geoffroy, L. Charlet, J. Pironon, Calcite precipitation from CO_2–H_2O–$Ca(OH)_2$ slurry under high pressure of CO_2, J. Crystal Growth 308 (2007) 228–236.
[25] G. Montes-Hernandez, D. Daval, R. Chiriac, F. Renard, Growth of nanosized calcite through gas–solid carbonation of nanosized portlandite particles under anisobaric conditions, Cryst. Growth Des. 10 (2010) 4823–4830.
[26] L.A. Gower, D.A. Tirrell, Calcium carbonate films and helices growth in solutions of poly(aspartate), J. Crystal Growth 191 (1998) 153–160.
[27] L. Pastero, E. Costa, B. Alessandria, M. Rubbo, D. Aquilano, The competition between $10\bar{1}4$ cleavage and $01\bar{1}2$ steep rhombohedra in gel growth calcite crystals, J. Crystal Growth 247 (2003) 472–482.
[28] Tang, E.J Elzingan, Y.J Lee, R.J. Reeder, Coprecipitation of chromate with calcite: batch experiments and X-ray absorption spectroscopy, Geochem. Cosmochem. Acta. 71 (2007) 1480–1493.
[29] G. Montes-Hernandez, P. Beck, F. Renard, E. Quirico, B. Lanson, R. Chiriac, N. Findling, Fast precipitation of acicular goethite from ferric hydroxide gel under moderate temperature (30 and 70 °C), Cryst. Growth Des. 11 (2011) 2264–2272.
[30] D.M. Roundhill, H.F. Koch, Methods and technique for the selective extraction and recovery of oxoanions, Chem. Soc. Rev. 31 (2002) 60–67.
[31] T.R. Harper, N.V. Kingham, Removal of arsenic from wastewater using chemical precipitation methods, Water Environ. Res. 64 (1992) 200–203.
[32] K.R. Fox, T.J. Sorg, Controlling arsenic, fluoride and uranium by point-of-use treatment, JAWWA 79 (1987) 81–84.
[33] L.E. Eary, D. Rai, Chromate removal from aqueous waste by reduction with ferrous iron, Environ. Sci. Technol. 22 (1988) 972–977.
[34] E.H. De Carlo, D.M. Thomas, Recovery of arsenic from spent geothermal brine by flotation with colloidal ferric hydroxide and long chain alkyl surfactants, Environ. Sci. Technol. 19 (1985) 538–544.
[35] F.F. Peng, D. Pingkuan, Removal of arsenic from aqueous solution by adsorbing colloid flotation, Ind. Eng. Chem. Res. 33 (1994) 922–928.
[36] S.K. Gupta, K.Y. Chen, Arsenic removal by adsorption, J. WPCF 50 (1978) 493–506.
[37] C.P. Huang, L.K. Fu, Treatment of arsenic (V) containing water by the activated carbon process, J. Water Poll. Control Fend. 56 (1984) 233–242.
[38] Y.K. Nakano, Takeshita, T. Tsutsumi, Adsorption mechanism of hexavalent chromium by redox within condensed-tanning gel, Water Res. 35 (2001) 496–500.
[39] G.M. Haggerty, R.S. Bowman, Sorption of chromate and other inorganic anions by organo zeolite, Environ. Sci. Technol. 28 (1994) 452–458.
[40] J.M. Zachara, C.E. Cowan, R.L. Schmidt, C.C. Ainworth, Chromate adsorption on amorphous iron oxyhydroxide in presence of major groundwater ions, Environ. Sci. Technol. 21 (1987) 589–594.
[41] M.M. Benjamin, Adsorption and surface precipitation of metals on amorphous iron oxyhydroxide, Environ. Sci. Technol. 17 (1983) 686–692.
[42] J.D. Peak, D.L. Sparks, Mechanisms of selenate adsorption on iron oxides and hydroxides, Environ. Sci. Technol. 36 (2002) 1460–1466.
[43] V.K. Gupta, V.K. Saini, N. Jain, Adsorption of As(III) from aqueous solutions by iron oxide-coated sand, J. Colloid Interface Sci. 288 (2005) 55–60.
[44] Derek. Peak, Adsorption mechanism of selenium oxyanions at the aluminium oxide/water interface, J. Colloid Interface Sci. 303 (2006) 337–345.
[45] B. Tomazic, R. Mohanty, M. Tadros, J. Estrin, Crystallization of calcium hydroxide from aqueous solution I. Preliminary study., J. Cryst. Growth 75 (1987) 329–338.
[46] G. Montes-Hernandez, A. Fernandez-Martinez, F. Renard, Novel method to estimate the linear growth rate of submicrometric calcite produced in a triphasic gas–liquid–solid system, Cryst. Growth Des. 9 (2009) 4567–4573.
[47] F. Gaboriaud, J.-J. Ehrhardt, Effects of different crystal faces on the surface charge of colloidal goethite (α-FeOOH) particles, Geochem. Cosmochem. Acta. 67 (2003) 967–983.